Synchronous Removal of Arsenic and Fluoride from Aqueous Solution: A Facile Approach to Fabricate Novel Functional Metallopolymer Microspheres

Anil R. Gupta, Vipin C. Joshi, Anshul Yadav, and Saroj Sharma*

ACCESS | Metrics & More | Article Recommendations | SI Supporting Information

ABSTRACT: Concurrence of arsenic (As) and fluoride (F^-) ions in groundwater is a serious concern due to their fatal effects. Herein, an attempt was made to fabricate quaternized poly(zirconyl dimethacrylate-*co*-vinylbenzyl chloride)] (ZrVBZ), a metallopolymeric microsphere in three-dimensional shape with a porous texture. The synthesized ZrVBZ was utilized for the synchronal removal of As and F^- from water. Techniques such as Fourier transform infrared spectroscopy, ^{13}C-nuclear magnetic resonance, scanning electron microscopy, and Brunauer−Emmett−Teller surface area were used to characterize the ZrVBZ. The maximum adsorption capacity of ZrVBZ for both fluoride and arsenic (q_{max} F^-: 116.5 mg g^{-1}, q_{max} As(V): 7.0 mg g^{-1}, and q_{max} As(III): 6.5 mg g^{-1}) at given experimental conditions (adsorbents' dose: 0.250 g L^{-1}, feed of F^-: 50 mg L^{-1}, As(V)/As(III): 2000 μg L^{-1}, and pH: 7.0 ± 0.2) was ascribed to the porous spherical architecture with dual functional sites to facilitate adsorption. The adsorption followed pseudo-second-order kinetics with a correlation coefficient of 0.996, 0.997, and 0.990 for F^-, As(V), and As(III), respectively. The isotherm data fitted to the Langmuir isotherm model, and the maximum capacity was 121.5, 7.246, and 6.68 mg g^{-1} for F^-, As(V), and As(III), respectively. The results of this study indicated that ZrVBZ could be used as an effective adsorbent for the simultaneous removal of F^-, As(V), and As(III) from an aqueous medium.
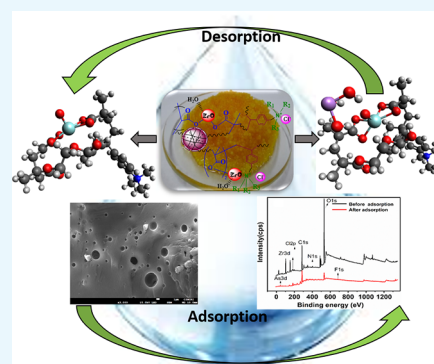
1. INTRODUCTION

Water is precious for the survival of life of all living beings.[1] It is reported that more than 80 countries and approximately 25% of the population around the globe have water severity and do not have adequate freshwater availability due to the presence of hazardous ions.[2] Among the various undesirable contaminants, fluoride and arsenic have been recognized as the most lethal and oncogenic elements available in groundwater.[3−5] Millions of people in different regions of the globe are suffering from arsenic's and fluoride's toxic effects.[6] Chronic exposure to arsenic-containing water can cause serious diseases, such as arsenicosis, while an excessive intake of fluoride-containing water causes dental and skeletal fluorosis.[7,8] The co-occurrence of both ions in water can abet a more lethal impact on an individual's health.[6] Thus, considering the severity of dual impact, removal of these ions from water is one of the most important steps in today's top priority water quality issue to prevent rather than treat diseases. Hence, it is important to focus on the removal of arsenic and fluoride from contaminated water. Several technologies exist for the removal of toxic contaminants, such as chemical precipitation,[9] adsorptive media,[10] ion exchange,[11,12] and membrane-based removal techniques,[13,14] i.e., electrodialysis, ultrafiltration, nano-filtration, and reverse osmosis. The adsorption process is the most feasible technique due to its vital features such as high efficacy, economic viability,

high throughput, simple operation and scaling up, etc.[15,16] In addition, the use of the adsorption technique also offers strategic advances in terms of water requirements and energy consumption.[15,16] Hence, a wide range of materials has been used to adsorb arsenic and fluoride from water such as neem, husk, rice, coconut shell char, tulsi, peel, bone char, activated carbon, fly ash, soils, and other geo-materials such as bauxite, zeolites, limestone, and alumina.[17,18]

The ability of transition metals to encounter toxic anions from water has been studied extensively owing to their electropositive behavior.[19] Hence, different metal-modified adsorbents using transition metals like Zn, Fe, Al, Ag, Zr, Ti, etc., have been widely explored for this purpose. These metal-modified adsorbents are mostly prepared by immobilizing metal ions (metal oxide/metal hydroxide) onto a solid support.[20−22] However, regardless of the preferable and faster uptake of ions, these aforementioned adsorbents suffer from few drawbacks: (i) there is low recovery after regeneration in case of the powder material; (ii) in many
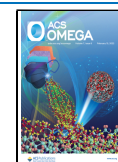
Table 1. The Characteristic Features of Microspheres of Varying Compositions[a]

s. no.	microsphere	ZrDMA (wt%)	VBC (wt%)	BET surface area (SA) (m^2 g^{-1}) (avg.)	pore volume (PV) (cm^3 g^{-1}) (avg.)	IEC (mequiv g^{-1})	ΦW	fluoride conc. (F^-) (mg L^{-1})	arsenic conc. As(V) (μg L^{-1})
1	pVBZ	00	100	253	0.21	2.5 ± 2.0	58.3 ± 2.0	1.6 ± 0.5	25 ± 1.0
2	ZrVBZ	50	50	421	0.36	3.7 ± 1.0	62.3 ± 1.0	0.8 ± 0.5	BDL
3	pZrDMA	100	00	452	0.44	nil	48.6 ± 1.0	0.4 ± 0.1	BDL

[a]Feed conc.: F^-: 10 mg L^{-1}, As(V): 250 μg L^{-1}, adsorbent's dose: 0.250 g L^{-1}, pH: 7.0 ± 0.2 for contact time of 3 h at 30 ± 2.0 °C. BDL: below detection limit (5.0 μg L^{-1}).

cases, the adsorbent's specific area drops due to pore blockage and immobilization of metal particles inside the pores; (iii) does not work well at extreme pH conditions;; (iv) release of immobilized metal ions from the solid support during adsorption into the water bodies; (v) in case of aluminium impregnated adsorbents, the release of aluminium is undesirable for the health due to neuro-toxic disorders such as Alzheimer's disease;[23] and (vi) the release of immobilized metal ions from the solid support during desorption is a cause of environmental problem due to sludge generation.[24]

Thus, considering the aforementioned drawbacks of conventional adsorbents, a modified approach has been attempted to fabricate a metallopolymeric network. Metallopolymers (MPs) are unique class of materials with significant interest in their large structural and chemical diversity due to tunable and desirable properties.

The MPs, comprising metal-containing monomers (MCMs) in their polymeric moiety, have been used in many fields such as the synthesis of optically active compounds, hydrogenation, hydroformylation, etc.[25] However, less reports are available for water remediation. Among several metals, zirconium is a better choice due to the superior electropositive behavior and better efficiency, which does not cause any toxic effect in the aquatic medium.[26,27] Moreover, the hydrated form of zirconium in the adsorbent stimulates improved removal of the anionic counterpart.[28] Thus, an attempt has been made to synthesize porous, cross-linked poly(zirconyl dimethacrylate-*co*-vinyl benzyl chloride) in 3D shape followed by functionalization with a quaternary ammonium group to get strong base anion functionality (ZrVBZ). The zirconium metal ion was anchored into the polymeric matrix by utilizing the presynthesized MCM of zirconyl dimethacrylate (ZrDMA) well before performing free radical polymerization. The prepared MP microsphere (ZrVBZ) was utilized as an adsorbent for the synchronous removal of arsenic and fluoride from water.

2. RESULTS AND DISCUSSION

2.1. Synthesis and Performance Study.
A series of porous and cross-linked metallopolymeric (MP) microspheres, i.e., ZrVBZ, was synthesized via the free radical polymerization technique. The proportion of co-monomers ZrDMA and VBC was varied to get the best microsphere, which has been used as an adsorbent for the removal of both arsenic and fluoride (Table 1). It has been observed that all the compositions of the polymeric microsphere were efficient to bring down both fluoride and arsenic concentration from an individual solution of both ions (Figure S1). However, the pZrDMA and ZrVBZ have been found to have be efficient and faster to remove both the ions compared to the pVBZ, which might be due to the higher surface area and porosity, favorable for the adsorption of ions. The highest surface area (SA: 452 m^2 g^{-1}) and porosity (PV: 0.44 cm^3 g^{-1}) were found in pZrDMA compared to pVBZ (SA:

253 m^2 g^{-1}, PV: 0.21 cm^3 g^{-1}) and ZrVBZ (SA: 421 m^2 g^{-1}, PV: 0.36 cm^3 g^{-1}), which might be due to the availability of zirconium in the polymeric structure that provides better porosity and surface area.[29] However, in the case of pZrDMA, the structural geometry (i.e., spherical shape) breaks down during use under stirring conditions. Hence, it has not been use for further study. Further, the presence of a metallic moiety along with the quaternary ammonium functionality in the same structure of ZrVBZ has been found to be better for the study compared to pZrDMA and pVBZ. Generally, it is observed that the presence of the strong anion functionalities in the polymer structure plays a dynamic role in the sorption of ions through the ion exchange process.[30] Thus, the movement of ions is affected by the presence of charge density through porous channels of the polymeric matrix. Thus, ZrVBZ was chosen for further elaborated studies.

2.2. Adsorbent's Structural, Morphological, and Thermal Characterization.
The structural and morphological properties of any polymeric network play an important role in adsorption behavior. Indeed, the adsorbent material's large surface area and pore volume impart a significant role in adsorption. The presence of zirconium ions in the 3D shaped ZrVBZ microsphere plays a strategic role to create pores, which support the passage of ions through porous channels.[29] Moreover, the presence of quarternary ammonium functionality ($-N^+R_3Cl^-$) in ZrVBZ provides a hydrophilic pathway to facilitate the movement of ions along with water molecules.[30] Thus, dual functionalities of ZrVBZ support the adsorption of arsenic and fluoride ions. The surface morphologies of ZrVBZ (pre- and post-adsorbed specimens) can be seen by SEM and EDX analysis conducted on the adsorbent by a field emission SEM (Supra VP40, Zeiss) instrument (Figure 1(i)). The well-developed porous structures with the smooth surface SEM image of spherical geometry ZrVBZ exhibit an average pore volume of 0.36 cm^2 g^{-1} and average pore size as 32 Å (Figure1(i)a,c). The EDX spectrum and electron mapping of the ZrVBZ showed the existence of both fluoride (d) and arsenic (e) after adsorption, indicating its co-adsorption efficacy. SEM–EDX imaging revealed no change in the morphology of ZrVBZ after adsorption. The SEM–EDX image revealed that % Cl ions has been reduced after anion adsorption from 6.74 to 3.77 wt%, which indicates the exchange of anion from the surrounding medium through the quaternary ammonium ($-N^+R_3Cl^-$) site.

Figure 1(ii) illustrates the FTIR spectra of ZrVBZ (pre-adsorbed, post-adsorbed, and regenerated specimens). The wide band at 3435–3458 cm^{-1} found in all the spectra can be jointly ascribed to the stretching vibration of the N−H and −OH group of the quaternary amine group ($-N^+R_3Cl^-$) and water of crystallization. Likewise, the frequencies at around 3030 and 2988–2932 cm^{-1} are ascribed to the C−H stretching vibrations of $-C_6H_5$, $-CH_3$, and $-CH_2$ of the polymer moiety. The small bands at 1478 cm^{-1} are assigned to $-N^+R_3Cl^-$ in the spectra of ZrVBZ.[31] Further, the stretching vibration band at 1725, 940,
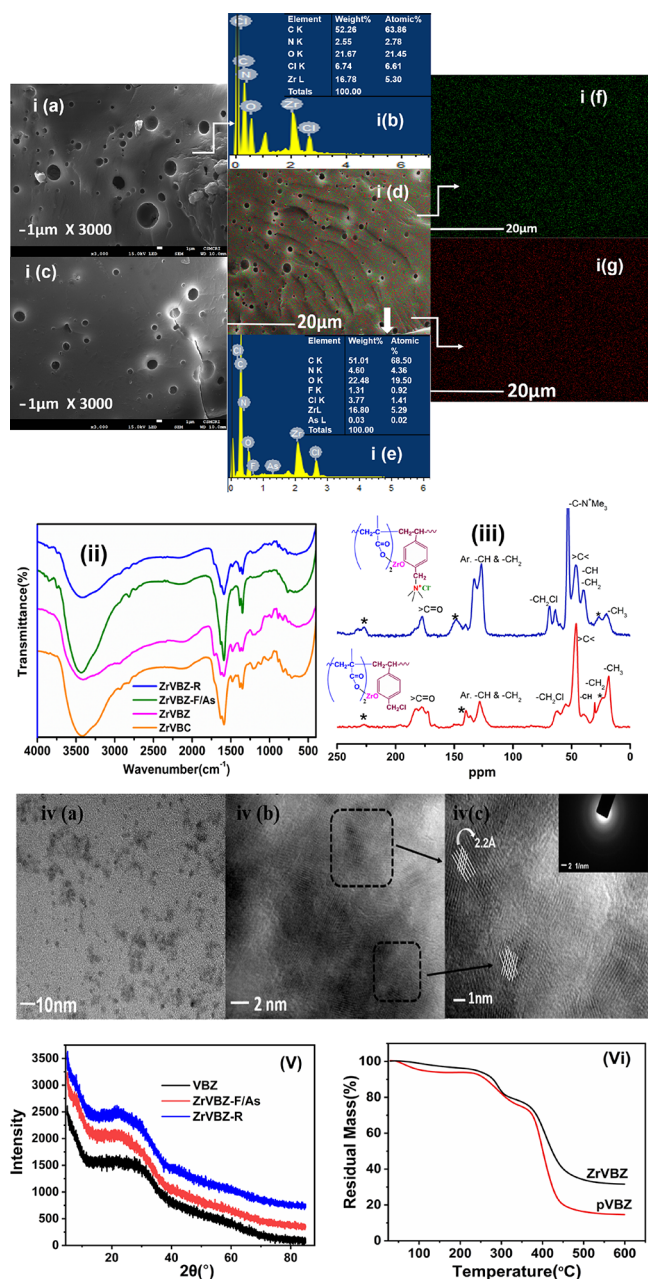
Figure 1. (ia,b) SEM and EDX analysis of pre-adsorbed ZrVBZ (1c−g) SEM and EDX analysis of post-adsorbed ZrVBZ. (ii) FTIR spectra of ZrVBZ: pre-absorbed, post-adsorbed, and regenerated. (iii) Solid-state ^{13}C-NMR of ZrVBC (pre-quaternized form) and ZrVBZ (post-quaternized form). (iv) TEM micrographs of ZrVBZ. (v) XRD spectra of pVBZ after adsorption (ZrVBZ-F$^-$/As) and after regeneration (ZrVBZ-R). (vi) TGA graph of pVBZ and ZrVBZ.

and 669 cm^{-1} corresponds to the carbonyl (>C=O), O−Zr−O, and Zr−O groups of ZrVBZ.[32] The absorption bands in the range of 1550−1400 cm^{-1} appeared due to symmetrical and asymmetrical −COO$^-$ vibrations. Further, the stretching vibration band at 1224, 1184−24, 897, and 830 cm^{-1} that can be ascribed to the >C=O (carbonyl), O−Zr−O, and Zr−O groups of ZrVBZ, respectively, may be owing to Zr atoms in two specific positions: coordinated with −O− and −OH groups. However, it is observed that after the adsorption, the intensity of these bands increased, which represents the possible adsorption of arsenic and fluoride through O−Zr−O---arsenic/fluoride.

Further, the exchange of chloride ions from the functional group (−N$^+$R$_3$Cl$^-$) of the adsorbent with fluoride ions of the surrounding medium is facilitated by ion-exchange phenomena. The identical spectra of ZrVBZ and ZrVBZ-R after regeneration again affirm no change observed in the polymeric matrix. Hence, it can be reused for sorption. Figure 1(iii) shows solid-state ^{13}C-NMR spectra of pre- (ZrVBC) and post-quaternized (ZrVBZ) forms of the microsphere. The spectrum of ZrVBC shows peaks at the chemical shift of 18.27, 30.2, 40.3, 46.0, 64−68, 176−177, and 126−133 ppm corresponding to aliphatic −CH$_3$, −CH$_2$, −CH, >C<, −CH$_2$Cl, and >C=O and aromatic carbons, respectively. On quaternization with TMA, a significant shift in the peak position of −CH$_2$Cl and aromatic >C< (attached with −CH$_2$Cl) groups is noticed, whereas other peaks remain almost at the same position. Upon reaction with TMA, the −CH$_2$Cl peaks shifted the peak downfield to ca. 63.7 ppm along with the appearance of a sharp peak at 53 ppm owing to −N$^+$R$_3$. Note that peaks shown with an asterisk are due to the spinning sidebands of aliphatic and aromatic peaks.

TEM images of ZrVBZ (Figure 1(vi)) revealed the presence of zirconium particles in the range of 3.0−6.0 nm, which is complementary to the particle size obtained by employing the Debye−Scherrer formula using XRD spectra. Well-resolved equidistant lattice fringes and a lattice space (*d*-spacing) of ∼2.0 Å are found with a lattice length of 2.2 Å. Wide peaks between 20 and 35 Φ in the XRD pattern of all the spectra indicate the amorphous nature of ZrVBZ. Moreover, the appearance of identical XRD patterns of all the forms (pre-adsorbed, post-adsorbed, and regenerated) is an indication of its stable matrix (Figure 1(v)).

The results of the thermal degradation trend of ZrVBZ and pVBZ adsorbents are depicted in Figure 1(vi). The presence of zirconium content in the polymeric moiety significantly influences the thermal stability of the adsorbents. It has been found that minor weight losses of 3.5 and 6.5% were observed with pVBZ and ZrVBZ, respectively, in the first decomposition phase up to ∼250 °C, which may be attributed to the loss of physically adsorbed water and/residual solvents entrapped in/on the surface of the adsorbent. The second phase of decomposition is observed due to degradation of a −C−C− and −N$^+$R$_3$Cl$^-$ functional moiety backbone chain of the polymeric microsphere. Further, complete thermal degradation occurred at ∼410 °C with weight loss of ∼60 and 45.77% for ZrVBZ and pVBZ, respectively. Residual masses of 34.05 and 16.24% were found with ZrVBZ and pVBZ at 500 °C, respectively.

3. ADSORPTION STUDY

3.1. Effects of Adsorbent Dosage. Investigating the adsorbent dosage to remove arsenic and fluoride is vital for getting the tradeoff between the adsorbent dose and the removal efficiency in an optimum adsorbent dose. Variable amounts of ZrVBZ were used to evaluate its performance in a mixed simulated solution of fluoride and arsenic with a fixed concentration. Two different sets of experiments have been carried out separately.

In the first set of experiment (F$^-$ + As(V)), the removal efficiency for both F$^-$ and As(V) increased rapidly from 40 to 68% and 70 to 97%, respectively with the increase in ZrVBZ dose from 0.05 to 0.15 gL^{-1} and reached 80 and 100% for F$^-$ and As(V), respectively, on further increase up to 0.2 gL^{-1}, whereas the equilibrium capacities (q_e F$^-$ and q_e As(V)) decreased from 80 to 36.8 mg g^{-1} and 3.5 to 1.0 mg g^{-1} for F$^-$ and As(V),
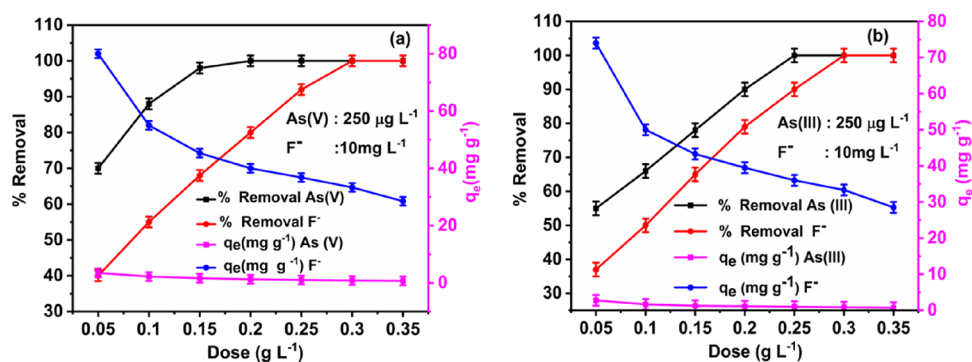
Figure 2. Performance of adsorbents of varying doses for the removal of fluoride and arsenic in mixed spiked solutions. (a) F$^-$: 10 mg L^{-1} + As(V): 250 μg L^{-1} and (b) F$^-$: 10 mg L^{-1} + As(III): 250 μg L^{-1} at pH: 7.0 $\pm$ 0.2, contact time: 3 h, temp.: 30 $\pm$ 2.0 °C, and rpm: 150.
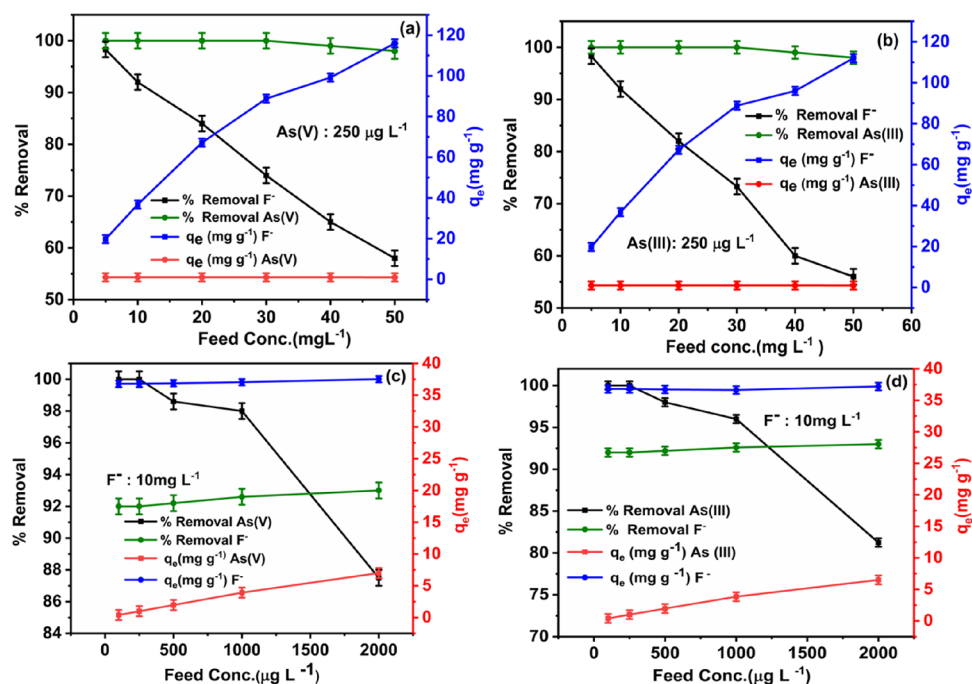
Figure 3. Performance of the adsorbent by varying feed concentrations of (a) F$^-$: 5.0−50.0 mg L^{-1} with fixed As(V) [250 μg L^{-1}], (b) F$^-$: 5.0−50.0 mg L^{-1} with fixed As(III) [250 μg L^{-1}], (c) varying concentrations of As(V) from 100 to 2000 μg L^{-1} with fixed F$^-$: 10.0 mg L^{-1}, (d) varying concentrations of As(III) from 100 to 2000 μg L^{-1} with fixed F$^-$: 10.0 mg L^{-1}, with a fixed dose of 0.250 g L^{-1}, pH: 7.0 $\pm$ 0.2, contact time: 3 h, temp.: 30 $\pm$ 2.0 °C, and rpm: 150.

respectively. On further increase in dose up to 0.25 g L^{-1}, the removal efficiency reached 88% (<1.5 mg L^{-1} F$^-$) for fluoride with 100% (<10 μg L^{-1}) arsenic removal, which is within the permissible limit of WHO for drinking water (Figure 2a). Further, in the next set of the experiments (F$^-$ + As(III)), similar trends were observed for both ions. Here, removal efficiencies for both F$^-$ and As(III) were found to increase from 40 to 80% with the increase in ZrVBZ dose from 0.05 to 0.20 g L^{-1}, which reached 90 and 100% on further increase up to 0.25 gL^{-1} for F$^-$ and As(III), respectively, whereas the equilibrium capacities (q_e F$^-$ and q_e As(III)) decreased from 74 to 36 mg g^{-1} for F$^-$ and 2.75 to 1.0 mg g^{-1} for As(III), respectively (Figure 2b), which are within the permissible limit of WHO for drinking water for both ions.

Thus, experimental results revealed that a very small amount of adsorbent's dose (0.250 g L^{-1}) was found to be efficient to bring down the concentration of both ions from their mixed solution to the WHO permissible limit, which would be useful for field applications where groundwater is contaminated with

both ions.[33] The increase in removal efficiencies for adsorbate with the adsorbent dose can be attributed to the availability of a high adsorbent−adsorbate ratio and greater adsorption sites, and an increase in diffusion path length due to the aggregation of the polymeric moiety. Once stabilized, no change could be observed due to the unavailability of free adsorption sites for ion binding.

3.2. Effects of Adsorbate Concentration. The effect of feed concentration on adsorption was studied with both arsenic and fluoride ions. The experiments were analyzed to evaluate the behavior of adsorbents in the presence of varying concentrations of one ion while keeping other ions at fixed concentrations. Four different sets of experiments were examined to evaluate the performance of ZrVBZ in the presence of both ions, where the concentration of one ion was varied. In contrast, the concentration of the other ion was kept fixed.

In the first two sets of the experiment, 100 to 98% removal efficiencies were found for both As(V) and As(III) in the presence of varying concentrations of fluoride (5.0−50 mg L^{-1})
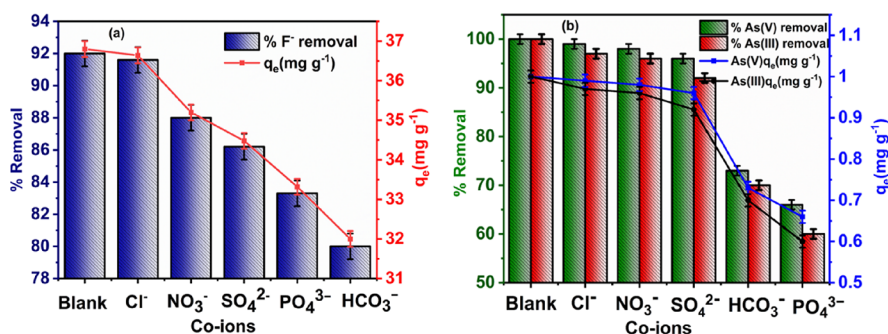
Figure 4. Effect of coexisting ions (a) F^-: 10.0 mg L^{-1} and (b) As(V): 250 μg L^{-1} + As(III) on the performance of the adsorbent.

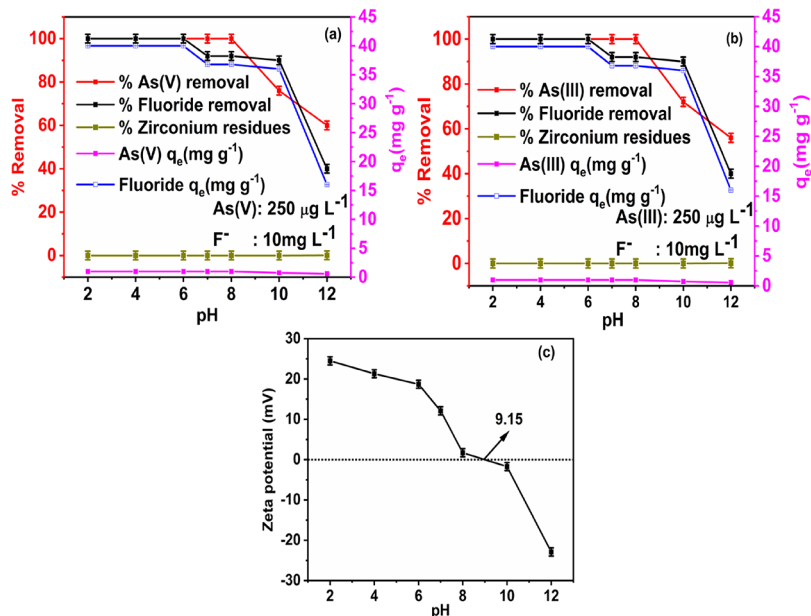**Figure 5.** Effect of pH on the adsorption of (a) F^-: 10.0 mg L^{-1} + As(V): 250 μg L^{-1} and (b) F^-: 10.0 mg L^{-1} + As(III): 250 μg L^{-1} on the performance of adsorbent; and (c) point of zero charge (PZC).

with equilibrium capacities (q_{max} As(V)/As(III)) of 0.98 mg g^{-1} for both forms of arsenic, whereas the % removal of fluoride decreased from 100 to 56% with the maximum adsorption capacities (q_{max} F^-) of 116.5 and 112 mg g^{-1}, respectively, in the presence of As(V) and As(III) separately (Figure 3a,b).

Further, in the next set of experiments, the % removal of fluoride increased rapidly from 92 to 93.8% and 92 to 93% in the presence of As(V) and As(III), respectively, with the feed concentration of 100−2000 μg L^{-1} (Figure 3c,d). The adsorption capacities of fluoride (q_{max} F^-) were found to be 37.52 and 37.2 mg g^{-1} in the presence of As(V) and As(III), respectively. In contrast to these results, 100% arsenic removal was found for both forms of arsenic up to 500 μg L^{-1}, which was further decreased to 87.5 and 81.2% As(V) and As(III), respectively, when the concentration was increased to 2000 μg L^{-1}. Thus, it has been found that both arsenic and fluoride can be successfully removed in the given set of experimental conditions up to the WHO permissible limit (F^-: 1.5 mg L^{-1} and As: <10 μg L^{-1}). This shows the synergic behavior of both ions with ZrVBZ.

Further, the ionic strength of one ion has the ability to affect the binding of the adsorbed species; it has been found that the presence of anions has a significant effect on the adsorption of As(V) while having a negligible effect on As(III). Hence, in the surrounding medium, F^- deteriorated the adsorption rate for

As(V), which might be attributed to the fact that these ions are monovalent with low ionic potential. It leads to a weaker competition ability with As(V). However, on the contrary, the % removal of fluoride increased in the presence of both forms of arsenic as concentration increased from 100 to 2000 μg L^{-1} in the present work. Moreover, in the reverse combination, a slight decrease (100−98%) in % removal efficiency of both forms of arsenic was found as fluoride concentration increased from 5.0 to 50.0 mg L^{-1}. Thus, a faster and more efficient adsorption is found using the ZrVBZ adsorbent, which shows the positive influence of one ion in the presence of another, which can be ascribed to the unique architecture of ZrVBZ with dual active sites. A huge specific surface area and well-developed pore structures provide an added benefit for ions' movement and the other ions.

3.3. Coexisting Ions on Adsorption. The effect of coexisting ions such as Cl^-, NO_3^-, SO_4^{3-}, PO_4^{3-}, and HCO_3^- on adsorption was studied. The literature revealed that chloride and nitrate ions form outer-sphere surface complexes; however, the sulfate ions form both inner- and outer-sphere surface complexes.[34]

Thus, sulfate ions have shown some extent of competing effects for removing fluoride and arsenic compared to the chloride and nitrate ions. At the same time, the fluoride removal efficiency is greatly affected by the bicarbonate alkalinity of the

water. It reduces the positive charge on the active sites of the adsorbent, which in turn decreases the efficiency of fluoride and arsenic removal. In the case of phosphate ions, it is adsorbed as an inner-sphere surface complex due to their high negative charge compared to other anions, which results in a decrease in the efficiency of arsenic adsorption by the adsorbent by interfering with arsenic.[35−37] In the coexistence of ions Cl^-, NO_3^-, SO_4^{2-} and PO_4^{3-}, and HCO_3^-, the percentage removal followed the order of 92, 91.6, 88, 86.2, 83.3, and 80% for fluoride ion; 100, 99, 98, 96, 73, and 66% for As(V); and 100, 97, 96, 92, 70, and 60% for As(III), respectively (Figure 4).

3.4. Effect of pH and PZC (Point of Zero Charge). pH is a crucial operational parameter that affects not only the surface charge of the adsorbent but also the degree of ionization and speciation of the adsorbate.[37] The removal of arsenic and fluoride was studied at different pHs of the solution ranging from 2.0 ± 0.2 to 12 ± 0.2 in two different sets of experiments as given in the experimental part (Figure 5a,b). The point of zero charge (PZC)/isoelectric point (IEP) of ZrVBZ measured by the zeta potential is pH 9.15, which indicates the positively charged surface up to this pH point (PZC) suitable for anion adsorption[38] (Figure 5c). Therefore, ZrVBZ showed good removal efficiency of ~92 and ~100% for fluoride and both arsenic ions (As(V)/As(III)), respectively, in the pH range of 6.0 ± 0.2 to 9.0 ± 0.2. Indeed, the 100% removal efficiency for all the three ions was observed in the pH range of 2.0 ± 0.2 to 6.0 ± 0.2, whereas the higher pH led to poor removal efficiency of ~40, ~60, and ~56% for fluoride, As(V), and As(III), respectively.

Generally, at lower pH, the metallic surface (Zr-OH) of the adsorbent gets protonated with a positive charge ($-Zr-^+OH_2$), while at basic pH, it is deprotonated with a negative charge ($-Zr-O^-$) (Figure 5).[39] Therefore, due to the presence of the protonated site in the acidic medium, the adsorption of anions was facilitated, with the possible formation of F-Zr-F, H_2O_3AsO-Zr-OAsO$_3H_2$, and H_2O_2AsO-Zr-OAsO$_2H_2$ with F^-, As(V), and As(III), respectively (Figure 6). At neutral pH, the removal of anions was achieved through Zr-OH groups, where surface is

neither protonated nor deprotonated. Under the higher pH range from 8.0 ± 0.2 to 12.0 ± 0.2, the removal of anions was significantly reduced, which might be due to the deprotonation of the Zr-OH site leading to the electrostatic repulsion between F^- and $Zr-O^-$ (Figure 6c). The speciation of arsenic is greatly dependent on the pH of the aqueous medium. Generally, arsenate exists as H_3AsO_4, $H_2AsO_4^-$, and $HAsO_4^{2-}$ forms in an oxidizing environment. The arsenate speciation $H_2AsO_4^-$ ions dominates in the pH range of 3.0 ± 0.2 to 6.0 ± 0.2, while $HAsO_4^{2-}$ dominates at a pH range of 8.0 ± 0.2 to 10.5 ± 0.2. However, both coexist in the intermediate pH range from 6.0 to 8.0. The arsenite speciation in an aqueous medium is controlled by $H_3AsO_3^0 \leftrightarrow H_2AsO_3^- + H^+$, p$K_a$ 9.2, in the pH range of 3.0 ± 0.2 to 11.0 ± 0.2. Though at pH 7.0 ± 0.1, the predominant arsenite species exist as uncharged $H_3AsO_3^0$,[40] it might get converted into As(V) in the presence of dissolved oxygen and light during sorption. On the other active site ($-N^+R_3Cl^-$), the adsorbent's surface is laden with a positively charged amino group in the acidic to neutral pH range from 2.0 ± 0.2 to 7.0 ± 0.2 to facilitate the adsorption of anions through positively charged nitrogen. Concomitantly, the exchange of anions from the surrounding medium was carried out through counter ions (Cl^-) of the ($-N^+R_3Cl^-$) functional site of ZrVBZ.[30] In the higher pH range, a strong interference of hydroxide ions could occur for both adsorption and ion exchange processes.[30]

To ensure the stability of the ZrVBZ microsphere at a wide range of pHs, the treated water samples were analyzed by ICP-MS to examine the presence of residual zirconium content. The results revealed a negligible amount of zirconium content in all the samples, which indicates the stability of prepared ZrVBZ over a wide range of pHs.

3.5. Desorption Study. To make the adsorption process an efficient and cost-effective process, the reusability of the adsorbent after regeneration is an important aspect of the study (Figure 7). Hence, it is a significant to re-use an adsorbent after multiple sorption/desorption cycles.[41]

Initially, different reagents such as HNO_3, NaCl, NaOH, and $NaHCO_3$ (0.1 M each) were used to examine the suitable eluting reagent for the desorption of F^-, As(V), and As(III) with individual solutions. The details of the experimental procedure performed in the study are given in the Supporting Information (SI). The % recovery of fluoride ions in HNO_3, NaCl, NaOH, and $NaHCO_3$ was 0, 32.5, 93, and 99.4%, respectively, while for As(V), it was found to be 8.0, 5.0, 90, and 75% and for As(III), it was 5.0, 2.5, 86, and 70%, respectively, in HNO_3, NaCl, NaOH, and $NaHCO_3$. Since the maximum desorption efficiency was found with the $NaHCO_3$ and NaOH solution for fluoride and arsenic, respectively, the cyclic desorption studies were carried out in the respective solutions. The desorption studies for all the ions were carried out for up to five cycles of use under given experimental conditions (the detailed information is given in SI S5). A slight decrease in efficiency was found in each cycle of operation, which might be due to experimental error (Figure S2a−c).

4. ADSORPTION KINETICS STUDY

4.1. Lagergren Pseudo-First-Order (PFO) and Pseudo-Second-Order (PSO) Kinetic Models. To investigate the adsorption kinetics of the ZrVBZ adsorbent, pseudo-first-order (PFO) and pseudo-second-order (PSO) models were employed. The PFO suggests that the rate of solute concentration variation with time and the variation in the adsorbent concentration and the quantity of adsorbate over time are
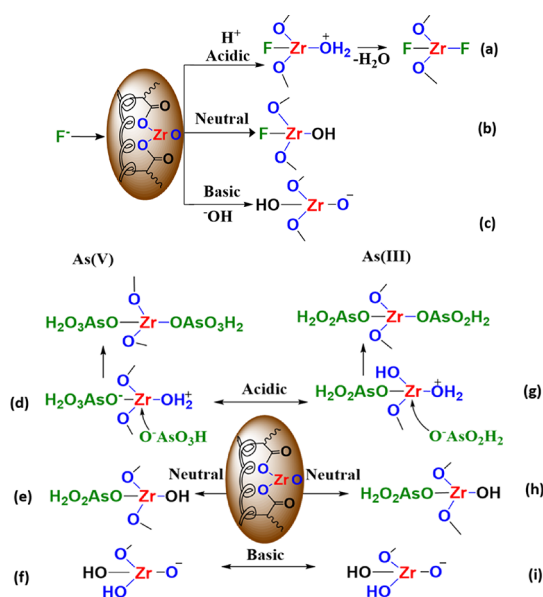

Figure 6. Schematic illustration of plausible adsorption interaction of F^- (a−c), As(V) (d−f), and As(III) (g−i) in different pH media.
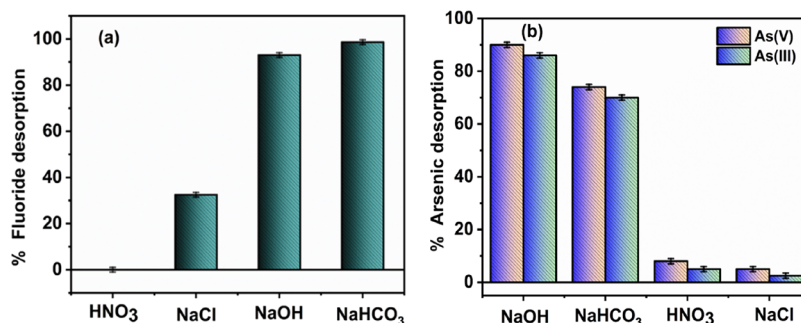
Figure 7. Desorption studies of ZrVBZ for (a) fluoride and (b) arsenic with an eluting reagent (0.1 M), contact time: 24 h, temp.: 30 ± 2.0 °C, and rpm: 150. F^-: 10 mg L^{-1} and As(V)/As(III): 250 μg L^{-1}.

Table 2. PFO and PSO Values for the Adsorption of Arsenic and Fluoride

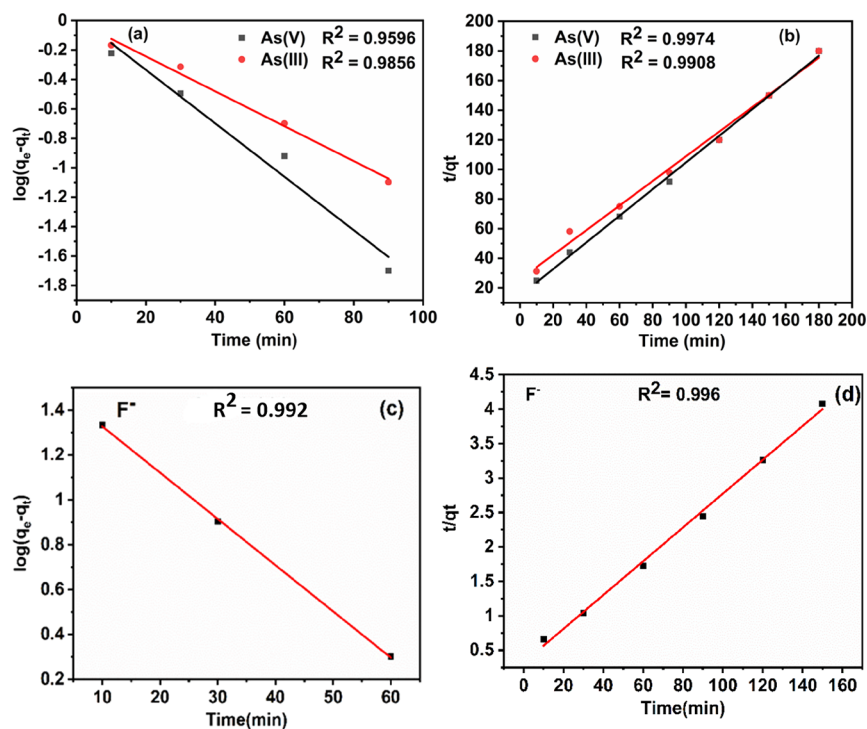| ions	PFO			PSO		
	K_1	q_e	R^2	K_2	q_e	R^2
F^-	0.0474	34.11	0.992	0.00000187	40.81	0.996
As(V)	0.0416	1.067	0.9596	0.0549	1.111	0.997
As(III)	0.0273	0.986	0.9856	1.2033	1.203	0.990

Figure 8. Pseudo-first-order (a, c) and pseudo-second-order (b, d) kinetic fits for As(V), As(III), and F^-.

logarithmically proportional, while PSO describes that the adsorption capacity of the adsorbent is directly proportional to the number of active sites engaged on it. The equations are represented as

$$\frac{dq_t}{dt} = K_1(q_{e-}q_t) \tag{1}$$

$$\frac{dq_t}{dt} = K_2(q_{e-}q_t)^2 \tag{2}$$

where q_t and q_e are the equilibrium adsorption capacities (mg g^{-1}) for the adsorption of fluoride/arsenic adsorbed at contact time t (min) and equilibrium, respectively, and K_1 (min^{-1}) and

K_2 (g mg^{-1} min^{-1}) are the pseudo-first-order and pseudo-second-order rate constant, respectively. The obtained values of PFO and PSO for the adsorption of both fluoride and arsenic are given in Table 2. The results revealed that the correlation coefficients (R^2) of the PSO model had a greater value (0.9974) than PFO (0.9696), and the calculated equilibrium capacity q_e ($q_{e\ theo}$: 1.0 mg g^{-1}) was found to be identical with the experimental one ($q_{e\ exp}$: 1.0 mg g^{-1}), which revealed that the kinetics of adsorption followed the PSO (Figure 8). The adsorption kinetics that followed the PSO indicate the possibility of the chemisorption process.[42]

Table 3. Adsorption Capacities of Different Bimetallic and Impregnated Metal Ion Modified Adsorbents for the Removal of Fluoride and Arsenic

| adsorbent | q_{max} (mg g^{-1}) | | | pH and initial concentration (mg L^{-1}) | | | ref |
	F$^-$	As(V)	As(III)	F$^-$	As(V)	As(III)	
AHNP	2.0	0.83		pH: 4.0 to 7.0 C_0: 10	pH: 7.0 C_0: 0.5		43
TLAC	80	28.5		pH: 5.0 C_0: 10	pH: 7.0 C_0: 30		44
CeFP	106.1	172.31		pH: 5.0 C_0: 37.9	pH: 5.0 C_0: 74.9		45
goethite	0.85	32.5		pH: 3.0 C_0: 25.60	pH: 5.0 C_0: 50.13		46
ZrMAg^{o}S	64	1.75		pH: 7.0 C_0: 5−50	pH: 7.0 C_0: 0.2−1		47
ARM	3.96	5.16	1.47	pH: 7.0 C_0: 2−30	pH: 7.0 C_0: 0.1−30	pH: 7.0 C_0: 0.1−30	48
hydrated cement	1.72	1.92		pH: 7.0 C_0: 30	pH: 7.0 C_0: 1		10
cellulose-g-PDMAEMA	8.5	27.93	8.96	pH: 7.0 C_0: 4	pH: 7.0 C_0: 10	pH: 7.0 C_0: 10	49
ZrVBZ	116.5	7	6.5	pH: 7.0 C_0: 5−50	pH: 7.0 C_0: 0.1−1	pH: 7.0 C_0: 0.1−1	present study
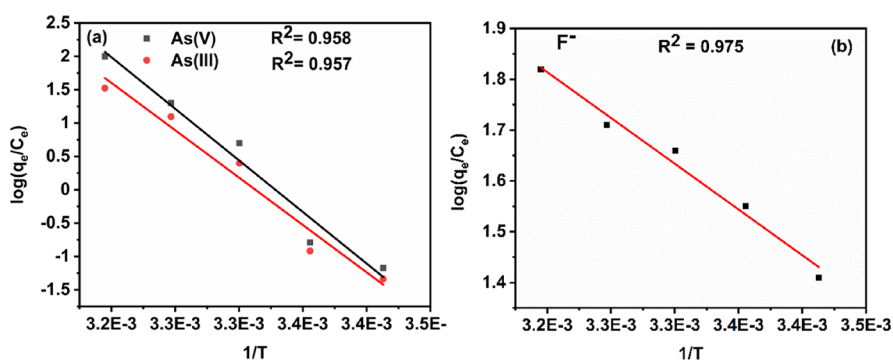
Figure 9. The plot of Gibbs free energy change $\Delta G°$ versus temperature (T) for (a) As(V) and As(III) and (b) fluoride.

5. ADSORPTION ISOTHERM STUDY

The adsorption isotherm is essential for describing the adsorption process for a solid−liquid system. The Langmuir and Freundlich isotherm models broadly utilize isotherms to represent the equilibrium distribution of the adsorbate onto the adsorbent (solid phase).

The following equation signifies the Langmuir isotherm in its linear form:

$$\frac{C_e}{q_e} = \frac{1}{b\,q_m} + \frac{1}{q_m}\,C_e \tag{3}$$

where b and q_{max} are Langmuir constants associated with the maximum adsorption capacity (mg g^{-1}) and adsorption energy, respectively. The values of b and q_{max} were obtained from the slope and intercept of the plot C_e/q_e versus C_e.

The Freundlich isotherm was commonly presented as follows:

$$\log q_e = \log K_f + \frac{1}{n}\log C_e \tag{4}$$

where q_e is the adsorbed ions of arsenic/fluoride at equilibrium (mg g^{-1}) and C_e is the concentration of arsenic/ fluoride at equilibrium. At the same time, K_f and n (as $1/n$) are Freundlich constants, representing the adsorption capacity (mg g^{-1}) and intensity of the adsorption, obtained from the slope and

intercept of the plot log q_e versus log C_e. The results in SI (Figures 3Sa−c and 4Sa−c and Table S1) indicated that the Langmuir isotherm model data well fitted with experimental data. The obtained experimental values are very close to the theoretical values ($q_{max\ theo}$), which signify the improved removal capability of both arsenic and fluoride ions by the developed ZrVBZ adsorbent with the specific conditions compared to several other adsorbents (Table 3).

6. THERMODYNAMICS STUDY

Another crucial factor that plays a vital role in adsorption is temperature. The effect of temperature on the adsorption by ZrVBZ is studied at five different temperatures, i.e., 293, 298, 303, 308, and 313 K. At the same time, other parameters were kept constant (adsorbent dose: 0.250 g L^{-1}, pH: 7.0 ± 0.2, rpm: 150, and contact time: 3 h). Results revealed that temperature has a positive effect on the adsorption of arsenic and fluoride. The equilibrium adsorption capacities (q_e) increased from 34.4 to 38.4 mg g^{-1} for fluoride, from 0.6 to 1.0 mg g^{-1} for As(V), and from 0.42 to 1.0 mg g^{-1} for As(III) on increasing temperature from 293 to 313 K with an initial feed concentration of F$^-$: 10.0 mg L^{-1} and As(V)/As(III): 250 μg L^{-1}. This performance indicates that both arsenic adsorption and fluoride adsorption are endothermic processes where temperature plays

Table 4. Thermodynamic Values, Gibbs Free Energy Change $\Delta G°$, ΔH, and ΔS for the Adsorption of F^- and As(V)/As(III)

| | ΔH (kJ mol^{-1} K^{-1}) | ΔS (kJ mol^{-1}) | ΔG (kJ mol^{-1}) | | | | |
			293	298	303	308	313
F^-	34.46	0.144	−7.99	−8.44	−9.43	−10.16	−10.88
As(V)	29.61	0.985	−28.84	−29.33	−29.83	−30.32	−30.81
As(III)	27.18	0.900	−26.36	−26.81	−27.26	−27.71	−28.14
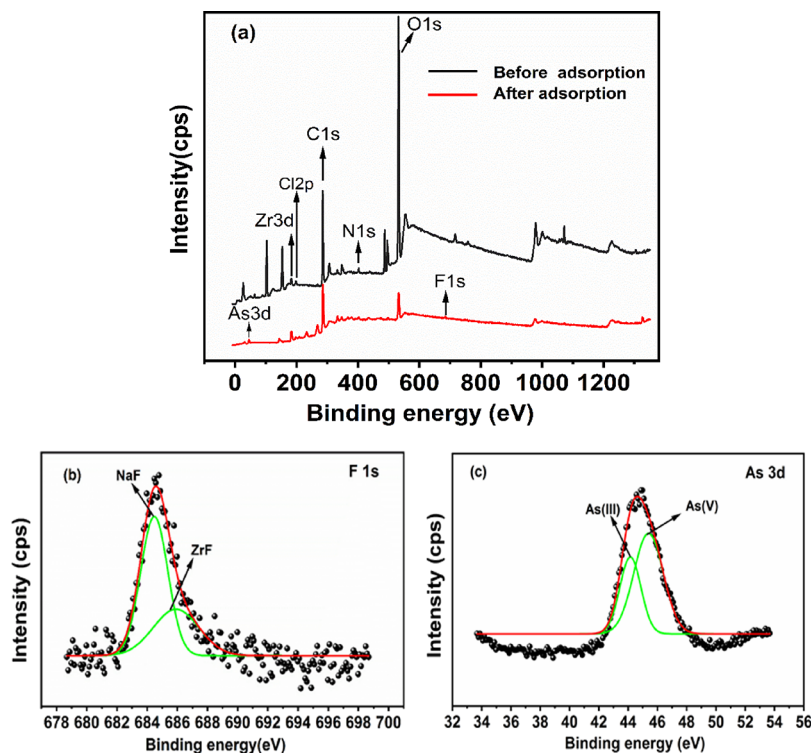
Figure 10. XPS spectrum of ZrVBZ. (a) Full spectrum before and after adsorption. (b) F^- spectrum. (c) As spectrum.

a key role. The van't Hoff equation is used to calculate the thermodynamic parameters of the adsorption process:

$$\log q_e/C_e = \frac{\Delta S}{2.303R} - \frac{\Delta H}{2.303RT} \quad (5)$$

$$\Delta G = \Delta H - T \times \Delta S \quad (6)$$

where R is a gas constant (8.314 J mol^{-1} K^{-1}), ΔS is the entropy change (J mol^{-1} K^{-1}), ΔH is the enthalpy change (kJ mol^{-1}), ΔG is the Gibbs free energy, and q_e/C_e is the adsorption affinity.

The ΔH and ΔS were obtained from the intercept and slope of the plot of log (q_e/C_e) vs $1/T$. The values of ΔH were found to be 29.61, 27.18, and 34.46 kJ mol^{-1} for As(V), As(III), and F^-, respectively. The values of ΔS were found as 0.985, 0.900, and 0.144 with regression coefficients (R^2) of 0.958, 0.957, and 0.975 for As(V), As(III), and F^-, respectively (Figure 9 and Table 4).

The positive values of both ΔH and ΔS suggest the endothermic and dissociative nature of the adsorption process. Moreover, the negative values of ΔG (−29.33, −26.81, and −11.44 kJ mol^{-1} at 298 K for As(V), As(III), and F^-, respectively) suggest the spontaneous and favorable adsorption process.[50]

7. XPS STUDY

The ZrVBZ has been used as an adsorbent for the removal of fluoride and arsenic ions from water. The adsorptive phenomena before and after adsorption are studied by XPS analysis. The full XPS spectra of the ZrVBZ adsorbent, before and after adsorption (Figure 10a), represented the absence and presence of fluoride and arsenic apart from other elements such as Zr, C, O, Cl, F, As, and N. The As (3d) spectrum of the arsenic sorbed adsorbent can be deconvoluted into two peaks, which usually originate from the different valent arsenic atoms and overlap each other.

In XPS, the As(V) is known to appear at higher binding energies in the species AsO_4^{3-} (44.9 eV), $HAsO_4^{2-}$ (45.5 eV), and $H_2AsO_4^-$ (46.7 eV), while As(III) appears at 44.0 eV.[51] Generally, the arsenite speciation in an aqueous medium is controlled by $H_3AsO_3^0 \leftrightarrow H_2AsO_3^- + H^+$ in the pH range of 3.0 to 11.0.[40] The presence of two peaks at binding energies of 45.5 and 44.0 eV can be assigned to the $HAsO_4^{2-}$ species of arsenate (As(V)) and $H_2AsO_3^-$ of arsenite (As(III)), respectively (Figure 10c).[52] This indicates the possible interaction of arsenic through the $H_2O_3AsO-Zr-OH$ and $H_2O_2AsO-Zr-OH$ complex with zirconium of the adsorbent, respectively. At the same time, the presence of two peaks in the fluoride spectra [F (1s)] at 684.5 and 685.35 eV can be ascribed to Na-F and Zr-F, respectively (Figure 10b).[53] The peak at 685.35 eV indicates that the possible interaction of fluoride with ZrVBZ could occur through OH-Zr-F formation at neutral pH during adsorption.

8. CONCLUSIONS

Herein, the present work reports a facile approach to fabricate a cross-linked, porous, and functional metallopolymer microsphere (ZrVBZ) in 3D shape. The methodology adopted to prepare such type of microsphere is unique to solve various demerits of conventional adsorbents due to its tunable structural composition with intact metallic moiety and tailorable porous texture. Physicochemical parameters were tuned to get the best suited microsphere anchored with intact metal ions along with the anion functionality, suitable for the synchronized removal of both ions from water. The unique architecture of ZrVBZ facilitated the synchronized sorption of fluoride and arsenic from water with the maximum adsorption capacities (q_{max}) of 116.5, 7.0, and 6.5 mg g^{-1} for F$^-$, As(V), and As(III), respectively, with the feed concentration of 50 mg L^{-1} for F$^-$ and 2000 μg L^{-1} for arsenic. The high practical utility of the ZrVBZ for the natural water environment contaminated with these ions can be evident from its superior efficiency (>96%) over a varied pH range.

9. EXPERIMENTAL SECTION

9.1. Materials. Methacrylic acid (MAA >99.8%), vinyl benzyl chloride (VBC >90.0%), ethylene glycol dimethacrylate (EGDMA >97.0%), and benzoyl peroxide (BPO >75.0%) were purchased from TCI Chemicals, Japan. The monomers were purified with basic alumina. The initiator benzoyl peroxide (BPO) was re-crystallized with methanol prior to use. Trimethylamine (TMA >98.0%), purchased from Central Drug House (CDH), India, was used as received. Sodium arsenate dibasic heptahydrate (Na$_2$HAsO$_4$·7H$_2$O), sodium arsenite (NaAsO$_2$), and sodium fluoride (NaF) were purchased from Sigma Aldrich, USA. Solvents, reagents, and salts such as toluene, acetone, methanol, hydrochloric acid, nitric acid, sodium hydroxide, sodium chloride, sodium nitrate, sodium phosphate, sodium sulfate, and sodium bicarbonate were procured from Fisher Scientific, India.

9.2. Fabrication of the ZrVBZ Adsorbent. Zirconyl dimethacrylate (ZrDMA), synthesized by a previously reported process, was used to fabricate adsorbents in a three-dimensional shape.[54] The cross-linked, porous adsorbent ZrVBC composed of ZrDMA and VBC of varying proportions was prepared by the free radical polymerization technique in the presence of a cross-linker (ethylene glycol dimethacrylate) and porogen (toluene). The detailed synthesis procedure is available in the SI.

After polymerization, the obtained ZrVBC microsphere was poured into an excess of trimethylamine in ethylene dichloride (TMA/EDC =80:20 v/v) at 50 ± 2.0 °C for 24 h under stirring (~50 rpm) to achieve the quaternary ammonium functionality onto the polymer moiety. The schematic illustration for the synthesis of the ZrVBZ microsphere is shown in Figure 11.

9.3. Characterization Techniques. The prepared ZrVBZ microsphere was characterized by different techniques. The details of instrumental analysis, such as FTIR, solid-state ^{13}C-NMR, SEM−EDX, TEM, XRD, ICP-MS, TGA, XPS, BET, zeta potential, and pH/ISE, are written in SI S3.

9.4. Adsorption Study. *9.4.1. Batch Adsorption Experiments.* A preliminary batch adsorption model was adopted to evaluate the performance of adsorbents of varying compositions (pVBZ, ZrVBZ, and pZrDMA) for the removal of F$^-$ and As from their simulated solutions with fixed experimental conditions, as follows: dose of adsorbent: 0.250 g L^{-1}, F$^-$: 10 mg L^{-1}, As(III): 250 μg L^{-1}, As(V): 250 μg L^{-1} at pH 7.0 ± 0.2,
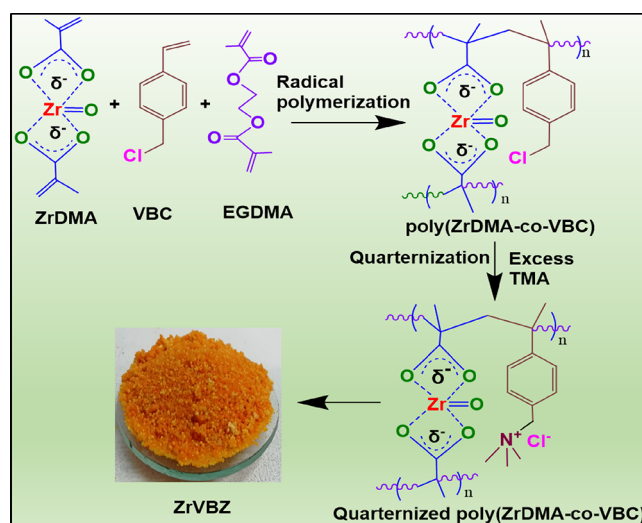

Figure 11. Schematic illustration for the synthesis of the ZrVBZ microsphere.

temp.: 30 ± 2.0 °C, and rpm: 150. Stock solutions of fluoride [F$^-$: 100 mg L^{-1}] and arsenic [As(III)/As(V): 1000 μg L^{-1}] were prepared from the salt of sodium fluoride, sodium arsenite, and sodium arsenate, respectively, in ultrapure water (water conductivity: 0.054 μS cm^{-1} at 30 ± 2.0 °C, resistivity: 18.2 Ωcm).

9.4.2. Effect of Adsorbent Dose on Adsorption. The effect of adsorbent dosage for removing F$^-$ and As is an important parameter to get the tradeoff between the adsorbent's dose and the removal efficiency. Variable amounts of ZrVBZ were used to evaluate its performance in mixed simulated solutions of fluoride and arsenic.

In the mixed solution, two different sets of experiments were performed to evaluate the optimum dose of the adsorbent to remove one ion in the presence of other ions. In the first set of experiments, F$^-$: 10 mg L^{-1} + As(V): 250 μg L^{-1}, and in second set of experiments, F$^-$: 10 mg L^{-1} + As(III): 250 μg L^{-1} were taken, while other parameters such as pH: 7.0 ± 0.2, contact time: 6 h and temp.: 30 ± 2.0 °C were kept constant.

9.4.3. Effect of Concentration Variation on Adsorption. The effect of feed concentration on adsorption was studied with both arsenic and fluoride ions. The experiments were analyzed to evaluate the behavior of adsorbents in the presence of varying concentrations of one ion while keeping other ions at fixed concentrations. Generally, a mixture of adsorbates exhibits three different types of behavior, i.e., (i) synergism (the effect of the mixture is greater than that of the single component in the mixture), (ii) antagonism (the effect of the mixture is less than that of each of the components in the mixture), and (iii) non-interaction (the mixture does not affect the adsorption of each of the adsorbents in the mixture).[55] In the present study, four different sets of experiments were performed to evaluate the adsorbent's performance in the presence of both the ions, where the concentration of one ion was varied while other ions were kept fixed. In the first two sets of experiment, F$^-$ was varied from 5.0 to 50.0 mg L^{-1} in the presence of fixed As(V) (250 μg L^{-1}) and As(III) (250 μg L^{-1}) separately, and in another two sets of experiments, As(V) and As(III) were varied separately from 100 to 2000 μg L^{-1} with a fixed F$^-$ concentration (10.0 mg L^{-1}), while other parameters, i.e., dose: 0.250 g L^{-1}, pH: 7.0 ± 0.2,

rpm: 150, contact time: 3 h, and temp.:30 ± 2.0 °C, were kept constant in all the experiments.

9.4.4. Effect of pH on Adsorption and Point of Zero Charge (PZC). The effect of pH on adsorption efficiency was studied by varying the pH of solutions ranging from 2.0 ± 0.2 to 12 ± 0.2 at fixed experimental conditions, such as adsorbent dose: 0.250 g L^{-1}, rpm: 150, contact time of 3 h, temp.: 30 ± 2.0 °C, and conc: F$^-$: 10 mg L^{-1}, As(III): 250 μg L^{-1}, and As(V): 250 μg L^{-1}. PZC is related to the charge on the surface of the particle and strongly depends on the pH of the material, so it influences a wide range of properties of colloidal materials, such as their stability, interaction with electrolytes, and ion exchange capacity. The point of zero charge of the ZrVBZ adsorbent sample has been determined using zeta potential measurement in the pH range 20 ± 0.2−120 ± 0.2. The results of zeta potential measurement are plotted as a function of pH.

9.4.5. Effect of Co-ions on Adsorption. The effect of co-ions on the remediation of fluoride and arsenic ions by the adsorbent was explored to have a better understanding of the adsorption process with 100 mg L^{-1} concentration of interfering ions such as chloride (Cl$^-$), nitrate (NO$_3^-$), sulfate (SO$_4^{2-}$), phosphate (PO$_4^{3-}$), and bicarbonate (HCO$_3^-$) under constant parameters, i.e., with the solution of 10 mg L^{-1} F^{-1} and As(III): 250 μg L^{-1}, As(V): 250 μg L^{-1}, at a fixed pH of 7.0 ± 0.2, contact time of 3 h with a dose of 0.250 g L^{-1}, and at temperature of 30 °C ± 2 °C. The initial pH values of the solutions in the presence of different co-existing ions were measured as 7.06 ± 0.1, 7.01 ± 0.1, 7.31 ± 0.2, 7.0 ± 0.2, and 8.10 ± 0.2 for Cl$^-$, NO$_3^-$, SO$_4^{2-}$, PO$_4^{3-}$, and HCO$_3^-$ ions, respectively.

9.4.6. Desorption and Regeneration Experiments. Any methodology that can bring down the operational cost with minimum maintenance would be more attractive and economical. Therefore, the sorption−desorption study was performed to examine the reusability of the prepared adsorbent. After investigating different eluting reagents to desorb fluoride and arsenic at fixed experimental conditions, the eluting reagents with the maximum desorption efficiency for the specific ions have been chosen for the study. NaOH and NaHCO$_3$ have been selected for the study due to the maximum desorption efficiency for arsenic and fluoride, respectively. The detailed description of the study is given in SI S5.

9.4.7. Physicochemical Characterization. The ion exchange capacity (IEC) was determined by the Volhard method. The IEC was obtained by the adopting the Volhard method.

The exchange of anions is calculated by the following equation:

$$\text{IEC (mequiv } g^{-1})$$
$$\frac{(\text{blank} - \text{sample})}{W_{\text{dry}}} = \times \text{ normality of KCNS} \times 10 \tag{7}$$

The water uptake of the adsorbent is calculated by immersing a specific quantity of the adsorbent (0.5 g) in DI water for 24 h by the following equation:

$$\text{Ø}w = \frac{W_{\text{wet}} - W_{\text{dry}}}{W_{\text{dry}}} \times 100\% \tag{8}$$

where W_{wet} and W_{dry} are the dry and wet weights of the adsorbent, respectively.

■ ASSOCIATED CONTENT

⑤ Supporting Information

The Supporting Information is available free of charge at https://pubs.acs.org/doi/10.1021/acsomega.1c05456.

> Synthesis of ZrVBZ; performance study; analytical measurements and methods for analysis; adsorption studies; desorption and regeneration study; and adsorption isotherm (PDF)

Accession Codes

The submitted work is original and has not been published elsewhere in any form or language.

■ AUTHOR INFORMATION

Corresponding Author

Saroj Sharma − *Membrane Science and Separation Technology Division, CSIR-Central Salt and Marine Chemicals Research Institute, Bhavnagar 364002 Gujarat, India; Academy of Scientific and Innovative Research (AcSIR), Ghaziabad 201002 Uttar Pradesh, India;* ⑩ orcid.org/0000-0002-7450-088X; Email: sarojs@csmcri.res.in

Authors

Anil R. Gupta − *Membrane Science and Separation Technology Division, CSIR-Central Salt and Marine Chemicals Research Institute, Bhavnagar 364002 Gujarat, India; Academy of Scientific and Innovative Research (AcSIR), Ghaziabad 201002 Uttar Pradesh, India*

Vipin C. Joshi − *Process Design and Engineering Division, CSIR-Central Salt and Marine Chemicals Research Institute, Bhavnagar 364002 Gujarat, India; Academy of Scientific and Innovative Research (AcSIR), Ghaziabad 201002 Uttar Pradesh, India*

Anshul Yadav − *Membrane Science and Separation Technology Division, CSIR-Central Salt and Marine Chemicals Research Institute, Bhavnagar 364002 Gujarat, India; Academy of Scientific and Innovative Research (AcSIR), Ghaziabad 201002 Uttar Pradesh, India*

Complete contact information is available at:
https://pubs.acs.org/10.1021/acsomega.1c05456

Author Contributions

Conceptualization: S.S.; Methodology: A.R.G., V.C.J, A.Y., S.S.; Formal analysis and investigation: A.R.G., V.C.J., A.Y., S.S.; Writing - original draft preparation: A.R.G., V.C.J., A.Y., S.S.; Writing - review and editing: A.R.G., V.C.J., A.Y., S.S.; Funding acquisition: S.S.; Resources: S.S.; Supervision: S.S.

Notes

The authors declare no competing financial interest.

■ REFERENCES

(1) Lee, A.; Elam, J. W.; Darling, S. B. Membrane materials for water purification: design, development, and application. *Environ. Sci.: Water Res. Technol.* **2016**, *2*, 17−42.

(2) Brookes, J. D.; Carey, C. C. Goal 6—rising to the challenge: enabling access to clean and safe water globally. *UN Chronicle* **2015**, *51* ().

(3) Ghosh, G.; Mukhopadhyay, D. K. Human health hazards due to arsenic and fluoride contamination in drinking water and food chain. In *Groundwater development and management*. Springer: Cham 2019, 351−369. DOI: 10.1007/978-3-319-75115-3_15.

(4) Amini, M.; Mueller, K.; Abbaspour, K. C.; Rosenberg, T.; Afyuni, M.; Møller, K. N.; Sarr, M.; Johnson, C. A. Statistical modeling of global geogenic fluoride contamination in groundwaters. *Environ. Sci. Technol.* **2008**, *42*, 3662−3668.

(5) Smedley, P. L.; Kinniburgh, D. G. A review of the source, behaviour and distribution of arsenic in natural waters. *J. Appl. Geochem.* **2002**, *17*, 517−568.

(6) Rao, M. V.; Tiwari, H. Amelioration by melatonin of chromosomal anomalies induced by arsenic and/or fluoride in human blood lymphocyte cultures. *Fluoride* **2006**, *39*, 255−260.

(7) Dibal, H. U.; Schoeneich, K.; Garba, I.; Lar, U. A.; Bala, E. A. Occurrence of fluoride in the drinking waters of Langtang area, north central Nigeria. *Health* **2012**, *04*, 1116−1126.

(8) Banerjee, A. Groundwater fluoride contamination: A reappraisal. *Geoscience Frontiers.* **2015**, *6*, 277−284.

(9) Turner, B. D.; Binning, P.; Stipp, S. L. S. Fluoride removal by calcite: evidence for fluorite precipitation and surface adsorption. *Environ. Sci. Technol.* **2005**, *39*, 9561−9568.

(10) Bibi, S.; Farooqi, A.; Hussain, K.; Haider, N. Evaluation of industrial based adsorbents for simultaneous removal of arsenic and fluoride from drinking water. *J. Cleaner Prod.* **2015**, *87*, 882−896.

(11) Pan, B.; Xu, J.; Wu, B.; Li, Z.; Liu, X. Enhanced removal of fluoride by polystyrene anion exchanger supported hydrous zirconium oxide nanoparticles. *Environ. Sci. Technol.* **2013**, *47*, 9347−9354.

(12) Patel, R. V.; Yadav, A. Photocatalytic MIL101 (Fe)/ZnO chitosan composites for adsorptive removal of tetracycline antibiotics from the aqueous stream. *J. Mol. Struct.* **2022**, *1252*, 132128. 1-16.

(13) Sharma, P. P.; Yadav, V.; Maru, P. D.; Makwana, B. S.; Sharma, S.; Kulshrestha, V. Removal of Fluoride from Brackish Water via Electrodialysis: An Environmentally Friendly Process. *ChemistrySelect* **2018**, *3*, 779−784.

(14) Yadav, A.; Indurkar, P. D. Gas Sensor Applications in Water Quality Monitoring and Maintenance. *Water Conserv. Sci. Eng.* **2021**, *6*, 175−190.

(15) Hao, L.; Liu, M.; Wang, N.; Li, G. A critical review on arsenic removal from water using iron-based adsorbents. *RSC Adv.* **2018**, *8*, 39545−39560.

(16) Habuda-Stanić, M.; Ravančić, M.; Flanagan, A. A review on adsorption of fluoride from aqueous solution. *Materials* **2014**, *7*, 6317−6366.

(17) Tamrakar, S.; Verma, R.; Sar, S. K.; Verma, C. cost effective natural adsorbents for the removal of fluoride: a green approach. *Rasayan J. Chem.* **2019**, *12*, 455−463.

(18) Asere, T. G.; Stevens, C. V.; Du Laing, G. Use of (modified) natural adsorbents for arsenic remediation: a review. *Sci. Total Environ.* **2019**, *676*, 706−720.

(19) Persy, V. P.; Behets, G. J.; Bervoets, A. R.; De Broe, M. E.; D'Haese, P. C. Lanthanum: a safe phosphate binder, *Semin Dial*, Blackwell Publishing Inc., Malden, USA, 2006; *19*(3), 195−199, DOI: 10.1111/j.1525-139X.2006.00169.x.

(20) Hernández-Maldonado, A. J.; Yang, F. H.; Qi, G.; Yang, R. T. Desulfurization of transportation fuels by π-complexation sorbents: Cu (I)-, Ni (II)-, and Zn (II)-zeolites. *Appl. Catal., B* **2005**, *56*, 111−126.

(21) Yadav, A; Sinha, N.; Organic Polymers for Drinking Water Purification. *Reference Module in Materials Science and Materials Engineering*, 2021. https://doi.org/10.1016/B978-0-12-820352-1.00140-1

(22) Kuwer, P.; Yadav, A.; Labhasetwar, P. K. Adsorption of cupric, cadmium and cobalt ions from the aqueous stream using the composite of iron(II,III) oxide and zeolitic imidazole framework-8. *Water Sci. Technol.* **2021**, *84*, 2288−2303.

(23) Tomljenovic, L. Aluminum and Alzheimer's disease: after a century of controversy, is there a plausible link? *J. Alzheimer's Dis.* **2011**, *23*, 567−598.

(24) George, S.; Pandit, P.; Gupta, A. B. Residual aluminium in water defluoridated using activated alumina adsorption − Modeling and simulation studies. *Water Res.* **2010**, *44*, 3055−3064.

(25) Pomogailo, A. D. May. (Co) polymerization of metal-containing monomers as a way of MMC synthesis. *Macromol. Symp.* **1998**, *131*, 115−125. Basel: Hüthig and Wepf Verlag.

(26) Sonal, S.; Singh, A.; Mishra, B. K. Decolorization of reactive dye Remazol Brilliant Blue R by zirconium oxychloride as a novel coagulant: optimization through response surface methodology. *Water Sci. Technol.* **2018**, *78*, 379−389.

(27) Jarvis, P.; Sharp, E.; Pidou, M.; Molinder, R.; Parsons, S. A.; Jefferson, B. Comparison of coagulation performance and floc properties using a novel zirconium coagulant against traditional ferric and alum coagulants. *Water Res.* **2012**, *46*, 4179−4187.

(28) Alagumuthu, G.; Rajan, M. Equilibrium and kinetics of adsorption of fluoride onto zirconium impregnated cashew nut shell carbon. *Chem. Eng. J.* **2010**, *158*, 451−457.

(29) Gupta, A. R.; Yadav, A.; Sharma, S. Scavenging fluoride from the aqueous system with porous organometallic three-dimensional architecture: An emerging adsorbent. *Environ. Sci. Pollut. Res.* **2021**, *28*, 19166−19178.

(30) Zhang, Q.; Du, Q.; Jiao, T.; Zhang, Z.; Wang, S.; Sun, Q.; Gao, F. Rationally designed porous polystyrene encapsulated zirconium phosphate nanocomposite for highly efficient fluoride uptake in waters. *Sci. Rep.* **2013**, *3*, 1−9.

(31) Lv, X.; Liu, C.; Song, S.; Qiao, Y.; Hu, Y.; Li, P.; et al. Construction of a quaternary ammonium salt platform with different alkyl groups for antibacterial and biosensor applications. *RSC Adv.* **2018**, *8*, 2941−2949.

(32) Kavaklı, P. A.; Güven, O. Güven, Removal of Concentrated Heavy Metal Ions from Aqueous Solutions Using Polymers with Enriched Amidoxime Groups. *Polym. Bull.* **2000**, *44*, 593−600.

(33) Chakraborti, D.; Rahman, M. M.; Chatterjee, A.; Das, D.; Das, B.; Nayak, B.; Pal, A.; Chowdhury, U. K.; Ahmed, S.; Biswas, B. K.; Sengupta, M. K.; Lodh, D.; Samanta, G.; Chakraborty, S.; Roy, M. M.; Dutta, R. N.; Saha, K. C.; Mukherjee, S. C.; Pati, S.; Kar, P. B. Fate of over 480 million inhabitants living in arsenic and fluoride endemic Indian districts: Magnitude, health, socio-economic effects and removal approaches. *J. Trace Elem. Med. Biol.* **2016**, *38*, 33−45.

(34) Onyango, M. S.; Kojima, Y.; Aoyi, O.; Bernardo, E. C.; Matsuda, H. Adsorption equilibrium modeling and solution chemistry dependence of fluoride removal from water by trivalent-cation-exchanged zeolite F-9. *J. Colloid Interface Sci.* **2004**, *279*, 341−350.

(35) Goldberg, S.; Sposito, G. A chemical model of phosphate adsorption by soils: I. Reference oxide minerals. *Soil Sci. Soc. Am. J.* **1984**, *48*, 772−778.

(36) Goldberg, S.; Sposito, G. A chemical model of phosphate adsorption by soils: II. Noncalcareous soils. *Soil Sci. Soc. Am. J.* **1984**, *48*, 779−783.

(37) Zhang, P. C.; Sparks, D. L. Kinetics and mechanisms of sulfate adsorption/desorption on goethite using pressure-jump relaxation. *Soil Sci. Soc. Am. J.* **1990**, *54*, 1266−1273.

(38) Wu, S.; Ge, Y.; Wang, Y.; Chen, X.; Li, F.; Xuan, H.; Li, X. Adsorption of Cr(VI) on nano Uio-66-NH2 MOFs in water. *Environ. Technol.* **2018**, *39*, 1937−1948.

(39) Singh, P.; Sarswat, A.; Pittman, C. U., Jr.; Mlsna, T.; Mohan, D. Sustainable low-concentration arsenite [As(III)] removal in single and multicomponent systems using hybrid Iron oxide−biochar nanocomposite adsorbents—a mechanistic study. *ACS Omega* **2020**, *5*, 2575−2593.

(40) Nordstrom, DK; Archer, DG. Arsenic thermodynamic data and environmental geochemistry. *In Arsenic in ground water.* Springer, Boston, MA, 2003; (p1−25).

(41) Singh, T.; Singhal, R. Reuse of a waste adsorbent poly (AAc/AM/SH)-Cu superabsorbent hydrogel, for the potential phosphate ion removal from waste water: Matrix effects, adsorption kinetics, and

thermodynamic studies. *J. Appl. Polym. Sci.* **2013** Sep 15, *129*, 3126−3139.

(42) Kumar, K. V.; Ramamurthi, V.; Sivanesan, S. Modeling the mechanism involved during the sorption of methylene blue onto fly ash. *J. Colloid Interface Sci.* **2005**, *284*, 14−21.

(43) Rathore, V. K.; Mondal, P. Competitive adsorption of arsenic and fluoride onto economically prepared aluminum oxide/hydroxide nanoparticles: Multicomponent isotherms and spent adsorbent management. *Ind. Eng. Chem. Res.* **2017**, *56*, 8081−8094.

(44) Jing, C.; Cui, J.; Huang, Y.; Li, A. Fabrication, characterization, and application of a composite adsorbent for simultaneous removal of arsenic and fluoride. *ACS Appl. Mater. Interfaces* **2012**, *4*, 714−720.

(45) Deng, H.; Yu, X. Adsorption of fluoride, arsenate and phosphate in aqueous solution by cerium impregnated fibrous protein. *Chem. Eng. J.* **2012**, *184*, 205−212.

(46) Tang, Y.; Wang, J.; Gao, N. Characteristics and model studies for fluoride and arsenic adsorption on goethite. *J. Environ. Sci.* **2010**, *22*, 1689−1694.

(47) Gupta, A. R.; Ranawat, B.; Singh, A.; Yadav, A.; Sharma, S. Zirconium-silver nano organo-bimetallic network for scavenging hazardous ions from water and its antibacterial potentiality: An environment-friendly approach. *J. Environ. Chem. Eng.* **2021**, *9*, 105356.

(48) Guo, H.; Yang, L.; Zhou, X. Simultaneous removal of fluoride and arsenic from aqueous solution using activated red mud. *Sep. Sci. Technol.* **2014**, *49*, 2412−2425.

(49) Tian, Y.; Wu, M.; Liu, R.; Wang, D.; Lin, X.; Liu, W.; Lin, M.; Li, Y.; Huang, Y. Modified native cellulose fibers—A novel efficient adsorbent for both fluoride and arsenic. *J. Hazard. Mater.* **2011**, *185*, 93−100.

(50) Jain, A.; Agarwal, M. Kinetic equilibrium and thermodynamic study of arsenic removal from water using alumina supported iron nano particles. *J. Water Process Eng.* **2017**, *19*, 51−59.

(51) Liang, J.-l.; Sun, W.-d.; Li, Y.-l.; Zhu, S.-y.; Li, H.; Liu, Y.-l.; Zhai, W. An XPS study on the valence states of arsenic in arsenian pyrite: implications for Au deposition mechanism of the Yang-shan Carlin-type gold deposit, western Qinling belt. *J. Asian Earth Sci.* **2013**, *62*, 363−372.

(52) Chowdhury, S. R.; Yanful, E. K.; Pratt, A. R. Arsenic removal from aqueous solutions by mixed magnetite−maghemite nanoparticles. *Environ. Earth Sci.* **2011**, *64*, 411−423.

(53) Cai, H.; Chen, G.; Peng, C.; Xu, L.; Zhang, Z.; Ke, F.; Wan, X. Enhanced fluoride removal by loading Al/Zr onto carboxymethyl starch sodium: synergistic interactions between Al and Zr. *RSC Adv.* **2015**, *5*, 101819−101825.

(54) Khan, H.; Gupta, A. R.; Sharma, S. Organometallic Adsorbent for Mitigating Fluoride from Water: An Environment-Friendly Approach. *ChemistrySelect* **2018**, *3*, 11765−11774.

(55) Girish, C. R. Multicomponent adsorption and the interaction between the adsorbent and the adsorbate: A review. *Interaction* **2018**, *14*, 15.